

Journal Pre-proofs

Research paper

Co-processed materials testing as excipients to produce Orally Disintegrating Tablets (ODT) using binder jet 3D-printing technology

Evelyn Ochoa, Lucia Morelli, Lucia Salvioni, Marco Giustra, Beatrice De Santes, Francesca Spena, Linda Barbieri, Stefania Garbujo, Matteo Viganò, Brian Novati, Giulia Tomaino, Saliha Moutaharrik, Davide Prosperi, Luca Palugan, Miriam Colombo



PII: S0939-6411(23)00313-2
DOI: <https://doi.org/10.1016/j.ejpb.2023.11.023>
Reference: EJPB 14158

To appear in: *European Journal of Pharmaceutics and Biopharmaceutics*

Received Date: 27 July 2023
Revised Date: 24 November 2023
Accepted Date: 27 November 2023

Please cite this article as: E. Ochoa, L. Morelli, L. Salvioni, M. Giustra, B. De Santes, F. Spena, L. Barbieri, S. Garbujo, M. Viganò, B. Novati, G. Tomaino, S. Moutaharrik, D. Prosperi, L. Palugan, M. Colombo, Co-processed materials testing as excipients to produce Orally Disintegrating Tablets (ODT) using binder jet 3D-printing technology, *European Journal of Pharmaceutics and Biopharmaceutics* (2023), doi: <https://doi.org/10.1016/j.ejpb.2023.11.023>

This is a PDF file of an article that has undergone enhancements after acceptance, such as the addition of a cover page and metadata, and formatting for readability, but it is not yet the definitive version of record. This version will undergo additional copyediting, typesetting and review before it is published in its final form, but we are providing this version to give early visibility of the article. Please note that, during the production process, errors may be discovered which could affect the content, and all legal disclaimers that apply to the journal pertain.

© 2023 The Author(s). Published by Elsevier B.V.

Co-processed materials testing as excipients to produce Orally Disintegrating Tablets (ODT) using binder jet 3D-printing technology

Evelyn Ochoa,^{1¶} Lucia Morelli,^{1¶} Lucia Salvioni,¹ Marco Giustra,¹ Beatrice De Santes,¹ Francesca Spina,¹ Linda Barbieri,¹ Stefania Garbujo,¹ Matteo Viganò,¹ Brian Novati,¹ Giulia Tomaino,¹ Saliha Moutaharrik,² Davide Prospero,¹ Luca Palugan^{2*}, Miriam Colombo^{1*}

¹University of Milano-Bicocca, Department of Biotechnology and Bioscience, Piazza della Scienza 2, 20126 Milano, Italy.

²University of Milano, Department of Pharmaceutical Science, Via Colombo, 71, 20133 Milano, Italy.

¶ These authors equally contributed.

* Correspondence to luca.palugan@unimi.it; miriam.colombo@unimib.it

Abstract

The use of co-processed materials for Orally Disintegrating Tablets (ODT) preparation by direct compression is well consolidated. However, the evaluation of their potential for ODT preparation by 3D printing technology remains almost unexplored. The present study aimed to estimate the use of commercially available co-processed excipients, conventionally applied in compression protocols, for the preparation of ODTs with binder jetting-3D printing technology. The latter was selected among the 3D printing techniques because the deposition of multiple powder layers allows for obtaining highly porous and easily disintegrating dosage forms. The influence of some process parameters, including layer thickness, type of waveform and spread speed, on the physical and mechanical properties of the prototypes printed were evaluated. Our results suggested that binder jetting-3D printing technology could benefit from the co-processed excipients for the preparation of solid dosage forms. The process optimization conducted with the experiments reported in this work indicated that additional excipients were needed to improve the physical properties of the resulting ODTs.

Keywords: 3D printing, Binder jetting, Orally Disintegrating Tablets, Co-processed excipients

1. Introduction

Orally disintegrating tablets (ODTs) are oral solid dosage forms that disperse almost instantly in the mouth and can be swallowed without needing water co-administration (1). Thanks to their ease of swallowing, ODTs are a valid and efficient alternative for medicines administration to some patients' categories such as geriatric (2,3), pediatric (3) or psychiatric patients (4), and for patients that suffer from dysphagia (5). ODTs can also be a valid alternative to improve gastric or duodenal absorption, to reduce the variability of transit through the pylorus or for active ingredients that act locally in the upper part of the digestive system. Furthermore, the ODT formulations can show better pre-gastric absorption avoiding first-pass metabolism and thus resulting in a faster onset (6).

Several approaches are used to prepare ODTs, including moulding, mass extrusion, freeze-drying and direct compression (7). The ODTs prepared with the latter two technologies are characterized by a higher porosity that allows a quicker disintegration when they come into contact with saliva. 3D printing technology, specifically the binder-jetting approach, can produce highly porous objects that could meet the physical and biopharmaceutical characteristics required for ODTs.

Recently, 3D printing technology has attracted a lot of attention due to its great potential and versatility. It is an additive manufacturing technique based on the principle of adding material layer upon layer to create an object. The use of 3D printing technology began in the 80s with the introduction of new printing techniques and materials with different physical and mechanical characteristics (8). This production technique has been developed in very different areas, such as the aerospace industry (9), construction and architecture (10,11) among others. In the healthcare area, 3D printing technology has found multiple applications, ranging from biomedicine (tissue engineering, surgical implants, prostheses, orthopaedics and dentistry) (12) to the production of surgical tools and in operative planning, providing imaging with higher resolution concerning 2D radiological imaging of patient anatomy (13,14). In pharmaceuticals, this technology has been employed for the preparation of modified-release forms including rapidly disintegrating and sustained-release devices (15,16).

The most used 3D printing methodologies in the pharmaceutical field are Fused Deposition Modelling (FDM), Semisolid Extrusion (SE), Material Jetting (MJ) and Binder Jetting (BJ) (17). Thanks to its versatility in developing structures in a few steps and using small amounts of actives and excipients, 3D printing offers some advantages over other standard approaches. This technology makes solid dosage forms easily accessible and readily available for clinical trials and personalized medicine, taking advantage of dose, shape and size customization (18). In BJ technology, a liquid binder is jetted onto a powder bed to induce powder agglomeration; it has some advantages over other 3D printing techniques. BJ technology makes use of raw materials already approved by regulatory agencies to prepare solid dosage forms and reduces material waste through feedstock recycling (19,20). This technique is appropriate for thermolabile substances since the printing takes place at room temperature and the objects can be dried at low temperatures. It is possible to choose whether to incorporate the active pharmaceutical ingredient into the solid mixture or to dissolve or suspend it in the binding liquid (21). Moreover, it is possible to obtain highly porous printed tablets, which makes them suitable for the preparation of dosage forms that disaggregate quickly. This technology shows some limitations: it is difficult to obtain dosage forms with appropriate mechanical properties suitable to withstand the stress to which they are subjected during packaging and handling; furthermore, the technology has low productivity and no widespread know-how. For these reasons, it does not represent a very appealing approach for the pharmaceutical industry at present. However, Aprelia Pharmaceuticals developed a fast-disaggregating tablet containing 1000 mg of levetiracetam, which was approved for commercialization by the FDA in 2015, under the trademark Spritam®. As far as we know, this product was the only pharmaceutical product approved for commercialization, manufactured with this technology (22).

The BJ printer machine comprises a binder solution reservoir connected to a print head, and two powder platforms: the feed platform, a powder reservoir, and the print platform, which is used to build the object (23) (Figure 1). A roller spreads a thin layer of powder from the feed platform to the print platform. In particular, the preparation method works by adding the powder material layer by layer to create the object. Between one layer and another, the binder solution is jetted from the printhead, which moves in the direction of the X-axis and Y-axis according to the product design data in the .stl file. The movement of the print platform along the Z-axis determines the layer thickness during printing. The powder layer's thickness will be set based on the desired resolution and strength of the printed object. The particle size of the powders should be smaller than the thickness of the layer to obtain objects with homogeneous density. However, it is necessary to take into consideration the problems deriving from the particle size of the powders during printing: coarse powders flow more easily but produce rougher surfaces and objects with less strength. Fine powders do not flow freely; thus, they can produce an inconsistent deposition of the powder in the printing platform, hence, a non-uniform layer density.

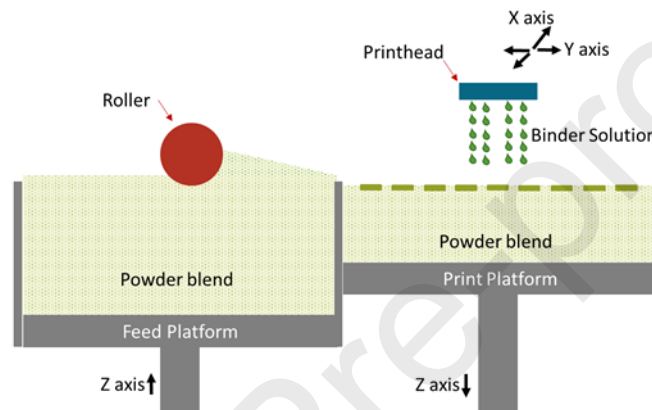


Figure 1. Schematic representation of inkjet-based 3D printing

BJ technology can be used with two different types of printhead: continuous inkjet (CIJ) or drop-on-demand (DOD). CIJ produces a continuous stream of droplets and the unused liquid is recycled. Differently, the DOD inkjet printer produces individual drops only when required. The drops are generated by a pressure pulse in a chamber placed behind the nozzle. This pressure can be induced by a thermal signal or by the most used piezoelectric transducer (24). The piezoelectric signal is represented by a graphic of voltage (V) as a function of time (μs), namely waveform (Figure 2). Upon emission of an electrical signal associated with the printhead output, the voltage rises and the piezoelectric element contracts, the time that the element remains contracted is the dwell time, which together with the rise time represents the pulse width (amplitude); during this time, a positive pressure is created which forces the ink out of the nozzle. The number of times this process repeats per second is the frequency (Hz). The range of frequency values depends on the type of printhead and is usually suggested by the manufacturer. The applied voltage controls the extent of nozzle membrane movement. At higher voltage, more solution is jetted from the nozzles. The waveform represents the signal that allows the binder solution to be jetted onto the powder through the nozzles and strongly influences the jetting process and the quality of droplets. To optimize the process, the waveform parameters such as pulse width (amplitude), pulse voltage and frequency can be adjusted depending on the liquid binder used (25).

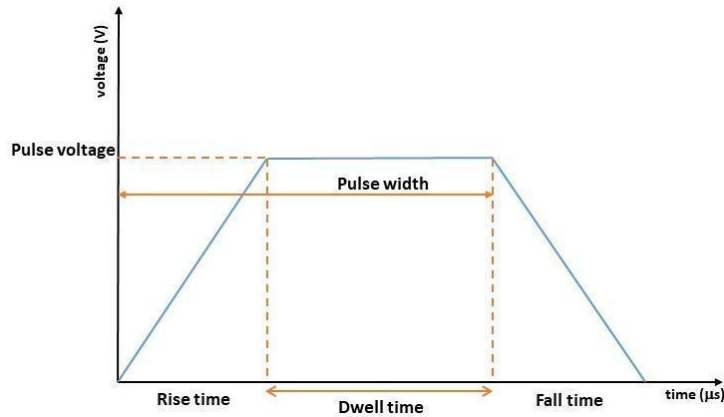


Figure 2. One pulse waveform diagram

The physicochemical properties of binder solution, such as surface tension, viscosity and density should be included in specific ranges for a correct “*jettability*” of the liquid from the printhead to generate reproducible single drops (in terms of size) that can reach the powder bed when required. The jet breakup behaviour of the fluids depends on the aforementioned properties and is evaluated by a dimensionless parameter namely Ohnesorge number (Oh) (25) which is calculated with equation 1:

$$Oh = \frac{\mu}{\sqrt{\rho R \sigma}} \quad (\text{Eq. 1})$$

Where μ , ρ and σ are the binder solution viscosity, density and surface tension, respectively, and R is the radius of the nozzle. The Ohnesorge number is often used to predict the printability of the droplets produced by the printhead. For binder solutions with an $Oh > 1$ the dissipative viscous forces avoid droplet formation, whereas, for $Oh < 0.1$, satellite drops that follow the main drop are formed. The impact of these drops on the solid surface can influence the resolution of the printed object.

Furthermore, the binder solution should be able to penetrate the powder bed, fill out the interstitial spaces and wet it. The degree of wettability of a solid can be measured by the contact angle, which is defined as the angle formed by the intersection of the liquid-solid-vapour interface. A less than 90° contact angle indicates that the solid surface is wettable. A contact angle greater than 90° means an unfavourable wettability (24).

As for the conventional technologies used for the preparation of solid dosage forms, also for BJ, the powders must have functionalities such as high bulk density, good flowability, good agglomeration properties and the ability to confer fast disintegration of the dosage form among others. No excipient possesses all these characteristics. Co-processed materials are blends of excipients that have undergone modifications in their physical structures without undergoing chemical changes. The co-processed excipients used for manufacturing tablets by direct compression are characterized by high bulk density, good flowability and compressibility (26). Co-processing is aimed at providing a new material with better functionalities compared to the physical blends of the components. In particular, co-processed excipients proposed for ODTs must be able to confer fast disintegration, good taste and pleasant mouthfeel (27).

This work aims to evaluate the feasibility of using co-processed excipients, commonly used for ODT manufacturing by direct compression, for the preparation of ODTs by binder jet 3D-printing technology. The impact of powder formulation and process parameters, such as layer thickness, type of waveform and extension speed on the overall quality of the prototypes printed was assessed in terms of their physical and mechanical properties (hardness, friability, disintegration time and shape).

2. Materials and methods

2.1. Materials

Powder blends were prepared with: GalenIQ™ 721 (GAL) (BENEO, D) or Ludiflash® (LUD) (BASF, D) or Pharmaburst® 500 (PHA) (SPI Pharma, USA), as ODTs co-processed excipients. Kollidon VA64 (KVA64) (BASF, D) was used as a polymer binder, then Aerosil® 200 (AER) (Evonik, D) (glidant) and mannitol (MAN) (Carlo Erba Reagents, I) (diluent) were also used.

GalenIQ™ 721 is a granulate of isomalt derived from beet sugar. Ludiflash® consists of four excipients: D-mannitol, crospovidone, polyvinyl acetate and povidone. Pharmaburst® 500 comprises mannitol, sorbitol, silicon dioxide and crospovidone. All co-processed are well known and are specific for the preparation of ODTs by direct compression (28).

For the liquid binder: povidone (Kollidon 30) (K30) (binder polymer), sodium lauryl sulfate (Kolliphor® SLS Fine) (SLS) (BASF, D) (surfactant), ethanol (ETH), glycerine (GLY) (humectant), propylene glycol (PPG) (Carlo Erba Reagents, I) (humectant) and deionized water (DEW) (Millipore, USA) were used.

2.2 Methods

2.2.1 Solid raw material characterization

Co-processed excipients (GalenIQ™, Ludiflash® and Pharmaburst®), Kollidon K30, Kollidon KVA64 and mannitol were preliminary evaluated for particle size distribution (Mastersizer 3000, equipped with a powder cell AEROS, software v3.81, Malvern Instruments Ltd, UK). D_{10} , D_{50} and D_{90} were calculated. D_x is the x-percentile of particle size distribution where x is the portion of particle with diameters smaller than D_x where x is: 10%, 50% or 90%. The bulk density was measured on about 100 g sample poured in a 250 mL glass cylinder, Carr's index was also determined (PT-TD300 Tapped density tester, Pharma Test, D).

2.2.2 Binder solution (Ink) preparation and characterization

A known amount of the binding polymer (K30) was added to water (DEW) and mixed until the polymer was completely solubilized. Then SLS and GLY (or PPG) were added and lastly the ethanol. The dispersion was filtered through a 5 μ m membrane and degassed. Table 1 shows the quali-quantitative composition (% w/w) of the binder solution.

Table 1. Quali-quantitative composition (% w/w) of binder solution

Ink Formulation	K30	GLY or PPG	SLS	ETH	DEW
(% w/w)	10	7	0.5	10	72.5

- Surface tension measurement

Capillary surface tension apparatus (Cole Parmer tensiometer, Cole Parmer, UK) was used to determine the binder solution's surface tension (mN/m) at 20 °C.

- Viscosity measurement

Viscosity at 20 °C (in mPa.s) was determined with a rotational viscometer (IKA Rotavisc, with an ELVAS-1 adapter, D) at rotational speeds from 30 to 60 rpm.

- *Density measurement*

A calibrated pycnometer of 25 mL (DIN Witeg, D) was used to determine the density of liquid binder samples. The mass of the tested sample was determined with an analytical balance (Radwag, mod. AS220.R2 Plus, D). Density at 20 °C was calculated as mass to volume (g/cm^3) ratio.

2.2.3 *Solid blend preparation and characterization*

250 g of powder blend for each batch was prepared in a Turbula® mixer (Willy A. Bachofen, Muttenz, CH) setting at 200 rpm for 10 min. Table 2 lists the composition of the blends.

The bulk density (about 100 g sample in a 250 mL glass cylinder) and Carr's index were determined (PT-TD300 Tapped density tester, Pharma test, D).

Table 2. Batches composition (% w/w) of solid blends

Powder blend formulation	GAL	LUD	PHA	KVA64	MAN
GAL+10%KVA64+40%MAN (GALb)*	50	-	-	10	40
LUD+10%KVA64+40%MAN (LUDb)	-	50	-	10	40
PHA+10%KVA64+40%MAN (PHAb)	-	-	50	10	40

*0.2% of AER was added to improve the powder flowability

2.2.4 *Prototype preparation*

The prototypes with a diameter of 5.0 mm and a height of 3.0 mm were designed by CAD software (AutoCAD 2021, Autodesk, USA) and loaded on the 3D binder jet printer (Armadillo White, Concr3de, NL) through the NOAH software, version 1.0 (Concr3de, NL). This software slices the 3D model in .stl format in layers according to an adjustable layer height. Each layer is a raster image saved in a specific folder, after generating the images each file is sent to the 3D printer. Each batch consisted of 100 units. The binder jet printer is equipped with a reduction insert intended for the manufacturing of small batches and integrated with a piezoelectric printhead (Fujifilm Dimatix Starfire SG1024/LA, J) with 1024 nozzles of 20 μm diameter. Three different waveforms were used in this work (Table 3). The drop weight for each waveform was calculated using Equation 3. Total weight is the mass of the binder jetted in a petri dish. Nozzle spitting time is the time that one nozzle jets the liquid binder.

$$\text{drop weight (ng)} = \frac{\text{total weight (ng)}}{1500 (\text{nozzle spitting times}) \times 1024 (\text{total nozzles in the printhead})} \quad (\text{Eq. 3})$$

Table 3. Variables setting of the different waveforms

Waveform	Width (μs)	Pulse (volts)	Freq (kHz)
Wf1	10	90	16.01
Wf2	13	120	18.69
Wf3	10	120	11.11 x 2*

*2 pulse waveform

After printing, the prototypes were carefully removed from the powder bed, de-dusted and dried at 35 °C for 15 hours (Memert, Mod. UF 55, D).

The process parameters studied were: a) layer thickness (0.1 mm or 0.2 mm), b) waveform type (Wf1, Wf2 and Wf3) and c) spread speed (10% or 40%). This is the speed at which the roller expands the powder on the printing surface.

To evaluate the influence of different process parameters on the physical and mechanical properties of the final product, different batches of prototypes were printed and then characterized by process yield, weight, physical aspect, disintegration time, crushing strength and friability.

- *Process Yield*

The process yield was calculated as the ratio between the number of undamaged prototypes obtained after de-dusted and their theoretical quantity (100) on the CAD file 3D model.

- *Tablet weight*



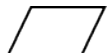
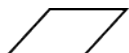
The weight of the tablets was determined on 20 samples for each batch using an analytical balance (Radwag, mod. AS220.R2 Plus, D). The mean and standard deviation were calculated.

- *Physical aspect*

An arbitrary numerical scale, from 0 to 3, was settled to assign the tablets' aspect (shape) with respect to the expected cylinder as shown in Table 4. Prototypes were photographed with a digital camera (Motorola, Edge 3, USA). The deformation of the tablets mainly concerns the inclination of the rectangle which constitutes its lateral projection and not the smoothing of the edges and vertices which mainly occurs with the manipulation of the prototypes.

Table 4. Arbitrary numerical scale to describe the shape of the tablets

Number	Cylinder form description	Schematic representation

0	regular form	
1	slightly warped	
2	very warped	
3	very deformed	
CD	completely deformed	

- *Prototypes dimensions*

The diameter and height of six prototypes for each batch were measured with a digital caliper (RM-SDM, Risemart, CN). Mean and standard deviation were calculated.

- *Disintegration time*

The test was performed in 800 mL of deionized water kept at $37.0\text{ °C} \pm 0.5\text{ °C}$, using a disintegration apparatus according to Ph. Eur. (2.9.1. Disintegration of tablets and capsules, Ph. Eur. 11.2 edition) (Pharma Test, mod. DIST-3, D).

- *Crushing strength*

The force required to break diametrically the tablets was determined using a dynamometer (Texture Analyzer, mod. TA.XTplusC, Stable Microsystems, UK) with a 5 mm diameter cylinder probe. Measurements were conducted in six replicates, for each batch, mean and SD values were calculated.

- *Friability*

To evaluate this characteristic, we set up a method to discriminate and evaluate the effects of the process parameters studied on the friability of the prototypes printed. The method used a vibrating sieve (mod. AS200 basic, Retsch, D) equipped with a 1.4 mm mesh sieve, at a fixed amplitude movement (60) for one minute. The friability was determined on six samples for each batch and was expressed in terms of the percentage of weight loss. This setup was used because the prototypes were very fragile and would not resist the mechanical stress produced for the apparatus described by Ph. Eur. (2.9.7. Friability of uncoated tablets, Ph. Eur. 11.2 edition).

3. Results

3.1 Solid raw material characterization

Based on the conclusion from previous works, which demonstrated that the properties of the powders strongly influence the quality of the printed product (29,30), we first performed a physical characterization

of the raw materials in terms of particle size distribution and bulk density (Table 5). The Carr's Index was calculated to evaluate powder flowability.

Table 5: Raw material characterization

Raw material	D ₁₀ (μm)	D ₅₀ (μm)	D ₉₀ (μm)	Bulk density (g/cm ³)	Carr's Index (%)
GalenIQ™	37.4 ± 0.1	113.0 ± 2.7	287.0 ± 12.4	0.456 ± 0.009	8.33 ± 0.35
Ludiflash®	29.4 ± 0.2	89.9 ± 0.9	483.0 ± 72.0	0.556 ± 0.004	9.30 ± 0.26
Pharmaburst® 500	37.1 ± 3.9	115.0 ± 10.5	254.0 ± 19.5	0.500 ± 0.002	8.00 ± 0.17
Kollidon® VA64	32.1 ± 0.2	85.9 ± 0.9	179.0 ± 2.8	0.372 ± 0.003	14.11 ± 0.64
mannitol	12.8 ± 0.1	66.7 ± 0.4	183.0 ± 0.8	0.566 ± 0.008	15.40 ± 1.09

Although all raw materials had a D₅₀ around 100 μm (the thickness of the thinnest prototype layer applied in this work), preliminary printing tests were carried out to evaluate the potential use of the materials without eliminating the larger particles. The tests gave encouraging results; particularly, co-processed excipients spread uniformly and although the prototypes prepared with them were weak and with rough surfaces, they still exhibited relatively narrow weight variations (RSD<5.0%) (data not shown). Therefore, it was decided to perform the next steps with the raw materials.

The co-processed excipients showed Carr's Index between 8% and 9%, confirming that they exhibited excellent flowability. Also, binder polymer (KVA64) and mannitol had good flowability, they showed Carr's Indexes lower than 16%.

3.2 Binder solution characterization

A preliminary study was performed (data not shown) to obtain a binder solution suitable to be used with the type of the selected print head. K30 was chosen, as a binding agent, for its well-known properties when used in solution to aid the aggregation of powder particles. Different polymer concentrations (between 5% and 15% w/w) were evaluated. The choice fell on the 10% w/w solution because its viscosity values were within those required by the print head. GLY and PPG were evaluated as possible humectant agents. The final choice fell on GLY which allows to obtain less fragile prototypes than those prepared with the binding solution containing PPG. Lastly, SLS was added to the binder solution selected (10% of K30 and GLY as humectant) to improve the wettability of powders. The binder solution was characterized in terms of viscosity, surface tension and density to verify if it was suitable for the printing process. To obtain good jetting performance, liquid binders must have physical characteristics within certain values that depend on the type of printhead used. Appropriate surface tension is necessary to produce well-formed drops, avoid the satellite drops and prevent the fluid from stagnating in the nozzle plate. Viscosity is a critical parameter that influences jetting

performance, and thus, the quality of the final object. The obtained values of surface tension, viscosity and density (Table 6) were used to calculate the Ohnesorge number ($Oh = 0.724$) which was within the suggested limits found in the literature for printheads similar to the one used in this work (25,31,32).

Table 6. Characterization of binder solution

Parameter	Experimental value
Surface tension	34.34 mN/m
Viscosity	13.56 mPa.s
Density	1.023 g/cm ³

3.3 Solid blend characterization

The bulk density and the flowability (Carr's Index) were measured to evaluate the suitability of the powder blend to be processed by the BJ-3D printer as well as any potential influence on the characteristics of manufactured prototypes. The results are shown in Table 7.

Table 7. Powder blend characterization

Formulation	Bulk density (g/cm ³)	Carr's Index (%)
GALb*	0.510 ± 0.006	16.9 ± 1.0
LUDb	0.535 ± 0.003	17.4 ± 1.4
PHAb	0.630 ± 0.007	11.7 ± 1.4

*0.2% of AER was added to improve the powder flowability

The bulk density values of the blends were very similar to each other; furthermore, they were sufficiently high to give the possibility of designing a dosage form of dimensions that were not excessively large. Although the powder mixtures showed higher Carr's index values compared to the relevant co-processed excipient, the flowability of all the blends was enough to be used to print the prototypes as we noticed in previous experiments (values within 18%) (Table 7).

3.3 Preparation of the printed tablets

3.3.1 Preliminary printing tests

	(%)	(mg) (mean ± sd)	aspect	Diameter (mean ± SD)	Height (mean ± SD)	(s)	(%)	(mean ± sd)	aspect	Diameter (mean ± SD)	Height (mean ± SD)	(s)
GALb*	87	29.9 ± 0.9	1	4.9 ± 0.1	3.0 ± 0.1	<1	99	34.0 ± 1.5	1	5.1 ± 0.1	3.0 ± 0.1	<1
LUDb	85	27.4 ± 1.0	1	4.8 ± 0.1	2.7 ± 0.1	<1	91	35.3 ± 2.4	1	5.2 ± 0.1	3.0 ± 0.1	<1
PHAb	87	25.8 ± 1.0	1	4.7 ± 0.1	2.6 ± 0.1	<1	92	30.5 ± 3.1	1	4.8 ± 0.1	2.6 ± 0.1	<1

*0.2% of AER was added to improve the powder flowability

**Disintegration time

The three batches manufactured with a 0.2 mm thickness layer showed a yield process equal to 85-87%. On the other hand, when the prototypes were prepared using a layer thickness of 0.1 mm, there was a notable enhancement in the process yield, obtaining values higher than 90% (Table 8). The average weight also increased because of the greater binder solution used to prepare the prototypes with 0.1 mm layers ($p < 0.05$). For all formulations, the prototype's morphology was slightly deviated from the expected cylindrical shape, as confirmed by the physical aspect score (see Table 4 in the Methods section). Furthermore, prototypes prepared with 0.2 mm layers showed very irregular surfaces ascribable to a material loss, probably due to insufficient binding solution. The disintegration time was very low, less than 1 s for all formulations regardless of the layer thickness used for their preparation.

The dimensions of the prototypes of the three batches printed with a 0.2 mm layer were similar to what was expected (5x3 mm). However, the dimensions of the prototypes prepared with LUDb and PHAb are slightly smaller. Only the difference between the dimensions of prototypes prepared with PHAb and the expected ones is significant ($p < 0.05$), probably because of the low mechanical properties of the tablets (Figures 3a, 3b and 3c) which tend to lose material when they are manipulated during characterization. Prototypes prepared with 0.1 mm layers showed a notable improvement in terms of mechanical properties in comparison with the batches prepared with 0.2 mm; an increase in crushing strength (Figure 3) was found for all formulations ($p < 0.05$). The increase in crushing strength for the prototypes containing GALb and LUDb was 10 and 8 times respectively. This result was expected since the amount of inkjet binder was doubled when the layer thickness was decreased from 0.2 mm to 0.1 mm. Although the formulations containing GALb and LUDb were still weak (crushing strength less than 6 N), the results of the friability test showed an important improvement (<1%). The prototypes obtained with PHA were weaker than the others. These results are surprising because the considered physico-technological characteristics are not very different among the three ODT excipients. Furthermore, we were not able to find other useful information, probably because these excipients are used for the preparation of tablets by direct compression, which does not involve intermediate wet granulation. In the formulation containing PHAb the increment of the hardness was very low but significant ($p < 0.05$), thus the prototypes resulted very weak in both layer heights evaluated. It could be hypothesized that the poor mechanical properties of PHAb depend on the absence of a substance with binding properties in the co-processed PHA, although the latter is capable of producing ODT with good mechanical properties by direct compression, to obtain formulations equally performing by 3D printing it may be necessary to change and/or increase the concentration of the binding agent. The PHAb prototypes prepared with 0.1 mm layer height showed a friability value of about 4%, much lower in comparison with that obtained for the prototypes

prepared with 0.2 mm layers (13.6%). The improvement of the mechanical properties of the prototypes leads to a greater yield process and dimensions of tablets closer to those expected.

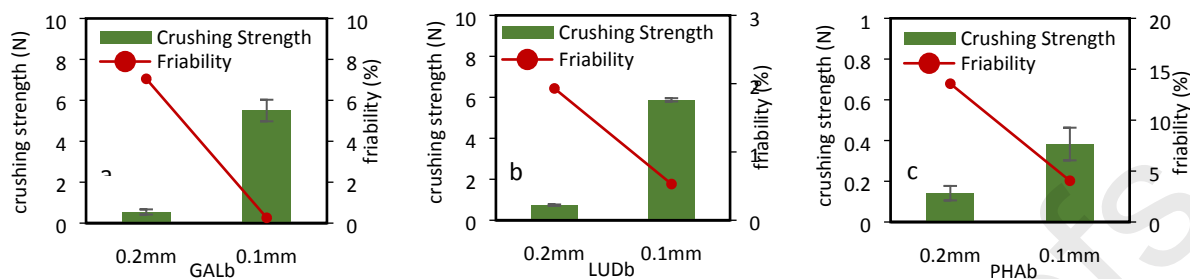


Figure 3. Influence of layer thickness in the mechanical properties of: 3a) prototypes containing GALb 3b) prototypes containing LUDb and 3c) prototypes containing PHAb

The particle size of the powders should be smaller than the thickness of the layer to obtain printed objects with homogeneous structures. However, it is also necessary to take into consideration the problems deriving from powder particle size during printing: coarse powders flow more easily but produce rougher surfaces and objects with less strength. Fine powders should not flow freely, producing an inconsistent deposition of the powder in the printing platform, and hence, a non-uniform layer density. Another problem that could arise connected to the particle size could be segregation; also, in this case, non-homogeneous structures could be produced even between printed tablets of the same batch.

Although the D_{50} of some raw materials used in this work was above the layer thickness, it was possible to prepare prototypes with suitable mechanical properties. These findings are consistent with some results found in the literature (29,33). The authors of those studies hypothesized that, especially in the case of hydrophilic and very water-soluble material, as the main material of co-processed excipients and mannitol used in this experimental work, the particles could undergo plastic deformation or partial dissolution when they come into contact with the binder solution, facilitating the homogeneous deposition of the subsequent layers until the final shape of the dosage form is achieved.

- Waveform Type

To improve the mechanical performances of the prototypes, in addition to the Wf1 (waveform default), two different waveforms able to produce larger drops were tested maintaining the layer thickness of 0.1 mm and the spread speed of 40%. The weight drop was calculated from Eq. 2. Also, the relevant amount of binder solution and solid material from binder solution (17.5% w/w of solid) used for the preparation of one tablet were calculated for the different waveforms. The results are shown in Table 9.

Table 9. Weight drop, amount of binder solution and solid material from binder solution calculated for a printed tablet slice 0.1 mm

Waveform	Weight drop (ng)	Binder solution (mg)	Solid from binder solution (mg)
Wf1	65.1	9.5	1.7
Wf2	71.6	10.5	1.8

Wf3	143.4	20.9	3.7
-----	-------	------	-----

Table 10 shows the results of the physical characteristics of prototypes prepared with GALb with different amounts of binder solution. The processes were performed by setting the thickness layer and the spread speed at 0.1 mm and 40%, respectively. Tablets prepared with Wf1 and Wf2 resulted in process yields above 90%, whereas Wf3 provided 51% yield. As expected, a greater amount of binder used to prepare the prototypes increased the average weight. However, a further increase in the binder used (Wf3) for the preparation of the prototypes produced an evident deformation of the tablet's shape. Around 49% of the prototypes printed were very deformed. In addition, they were disrupted when removed from the powder bed, which explains the low efficiency of the printing process.

As expected, an improvement in the crushing strength of prototypes containing GALb was reached when the waveform type was changed from the default form (Wf1) to waveforms that jetted greater amounts of binder solutions (Wf2 and Wf3) resulting in significant differences ($p < 0.05$). Nevertheless, increasing the amount of jetted binder solution leads to slightly higher friability values, which, in any case, were less than or very close to 1% (Figure 4). At the moment we have not found an explanation for this behavior. Although this trend is quite fair, it could be studied more in-depth in the following steps of the research project. GALb formulations prepared with Wf2 and Wf3 had good mechanical strength (hardness higher than 25 N), and disintegration times that exceeded 60 s. However, these values were always within the limits required by the European Pharmacopoeia (180 s) (2.9.1. Disintegration of tablets and capsules, Ph. Eur. 11.2 edition) (Table 10). The score shapes of the prototypes prepared with Wf1 and Wf2 were 1 and 0 respectively. Prototypes prepared with Wf3 had a completely deformed shape probably due to an excess of liquid binder permeating the powder layer, which was not able to absorb all the jetted solution before a new layer was spread.

Increasing the amount of jetted binder solution, the prototypes resulted more deformed. This trend occurs for all three formulations, but it is more evident for GALb. We hypothesized that this behaviour could be ascribed to the greater quantity of water which could increase the mobility of the particles due to the lubricating action of water. Otherwise, when the amount of binder solution jetted is low, and thus the amount of water, the mechanical properties of printed prototypes are fairer. The differences between the dimensions of the prototypes prepared with Wf1 and Wf2 were significant ($p < 0.05$). The dimensions of the prototypes prepared with Wf3 were not measured because of the irregular form of the tablets printed.

Table 10. Comparison of physical properties of GALb prototypes prepared with different waveforms

Waveform type (mg of solid binder)	Yield (%)	Weight (mg) (mean \pm SD)	Physical aspect	Dimensions (mm)		DT* (s)
				Diameter (mean \pm SD)	Height (mean \pm SD)	
Wf1 (1.66)	99	34.0 \pm 1.5	1	5.1 \pm 0.1	3.0 \pm 0.1	<1
Wf2 (1.84)	95	46.9 \pm 4.6	0	4.8 \pm 0.1	3.4 \pm 0.2	78
Wf3 (3.67)	51	50.5 \pm 5.9	CD	-	-	86

*Disintegration time

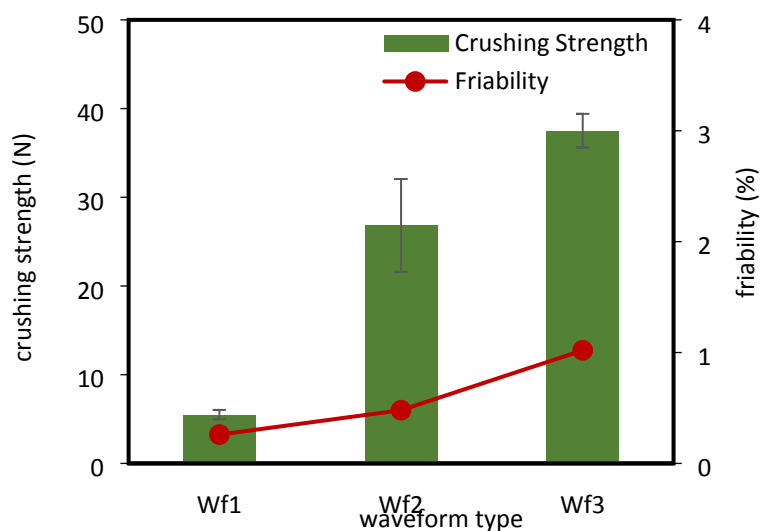


Figure 4. Influence of waveform type on the mechanical properties of GALb prototypes

Table 11. Comparison of physical properties of LUDb prototypes prepared with different waveforms

Waveform type (mg of solid binder)	Yield (%)	Weight (mg) (mean \pm SD)	Physical aspect	Dimensions (mm)		DT* (s)
				Diameter (mean \pm SD)	Height (mean \pm SD)	
Wf1 (1.66)	91	35.3 \pm 2.4	1	5.2 \pm 0.1	3.0 \pm 0.1	<1
Wf2 (1.84)	95	39.5 \pm 1.7	1	5.3 \pm 0.1	3.0 \pm 0.2	3
Wf3 (3.67)	100	44.3 \pm 2.7	2	5.4 \pm 0.2	3.0 \pm 0.3	<1

*Disintegration
time

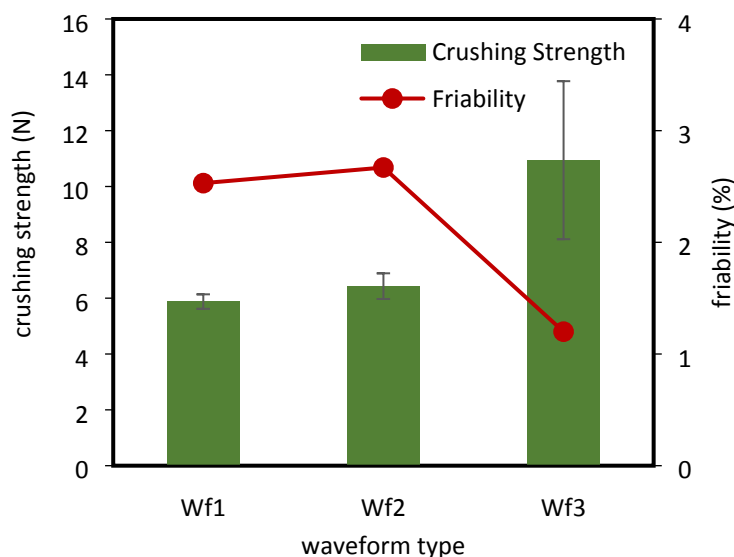


Figure 5. Influence of waveform type on the mechanical properties of LUDb prototypes

As with GALb prototypes, an improvement in process yield and an increase in average weight were found in LUDb prototypes printed with 0.1 mm of layer thickness and 40% spread speed. Also, the shape deformation increased when the amount of binder solution was increased. Instead, the disintegration time is very low (less than 3 s) in all formulations (Table 11). There were no differences ($p < 0.05$) between the dimensions of the tablets prepared with LUDb using different amounts of binder solutions. LUDb prototypes printed with Wf1 and Wf2 exhibited similar crushing strengths and friability ($p > 0.05$) (Figure 5). This could indicate that the amount of binder jetted using Wf2 was not sufficient to improve the mechanical resistance of the prototypes. However, a further increase in the solution (Wf3) produced an improvement in the quality of the prototypes: the friability was near 1% and the crushing strength was very variable with a mean of about 10 N.

Table 12. Comparison of physical properties of PHAb prototypes prepared with different waveforms

Waveform type (mg of solid binder)	Yield (%)	Weight (mg) (mean \pm SD)	Physical aspect	Dimension		DT* (s)
				Diameter (mean \pm SD)	Height (mean \pm SD)	
Wf1 (1.66)	92	30.5 \pm 3.1	1	4.8 \pm 0.1	3.0 \pm 0.1	<1
Wf2 (1.84)	91	36.7 \pm 3.8	3	4.8 \pm 0.0	3.0 \pm 0.1	<1
Wf3 (3.67)	100	54.4 \pm 7.4	3	4.8 \pm 0.1	3.2 \pm 0.1	<1

*Disintegration time

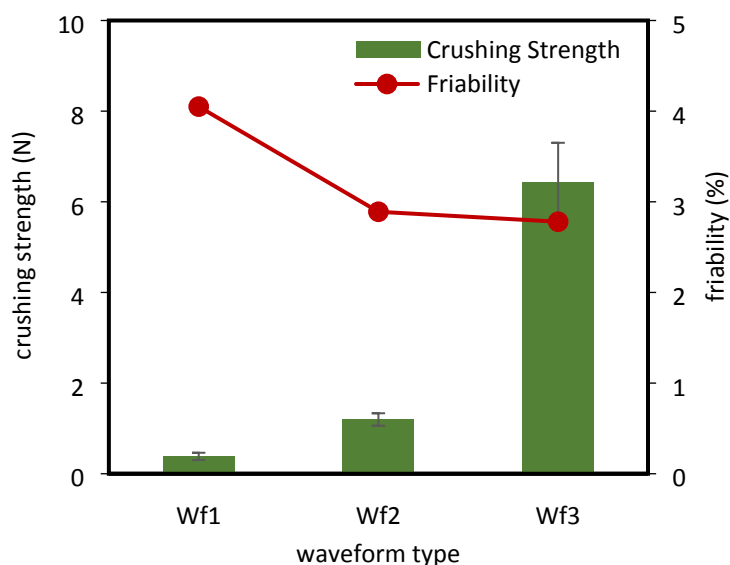


Figure 6. Influence of waveform type on the mechanical properties of PHAb prototypes

For PHAb prototypes, printed with 0.1 mm of layer thickness and 40% spread speed, an increase in weight was observed when a greater amount of binder solution was used (Table 12). There were no significant differences ($p < 0.05$) between the dimensions of the tablets prepared with PHAb when the amount of binder solutions was increased. The change in the waveform results in significant improvements in the breaking strength of the prototypes ($p < 0.05$). However, the increase in binder solution was not enough to obtain prototypes with good mechanical properties. All PHAb formulations had crushing strength below 10 N and friability above 3% (Figure 6).

- Spread speed

The spread speed is the speed of the roller which spreads the layer of powder in the printing. In NOAH, the software of Armadillo 3D print, it is expressed as a percentage of the maximum achievable speed, which is 100%.

Figure 7 shows the prototypes of two different batches prepared with GALb solid blend. The process parameters were fixed to 0.1 mm layer thickness and waveform Wf3. The prototypes on the left photo (7A) were printed with a spread speed of 40%, and corresponds to the formulation discussed above, while the ones on the right photo (7B) were printed with a speed of 10%, their shapes corresponded to number CD and 3 in the arbitrary scale (Table 4) respectively. The decrease in spread speed improved the shape of the prototype but not enough to be considered an “acceptable” shape.

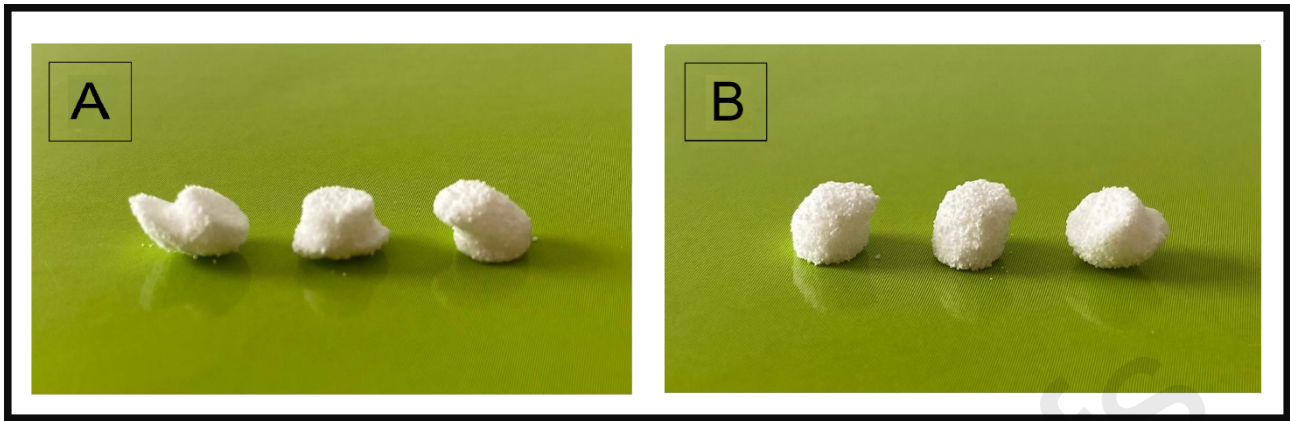


Figure 7. Influence of spread speed on the shape of the prototype GALb. A= 40%, B= 10%

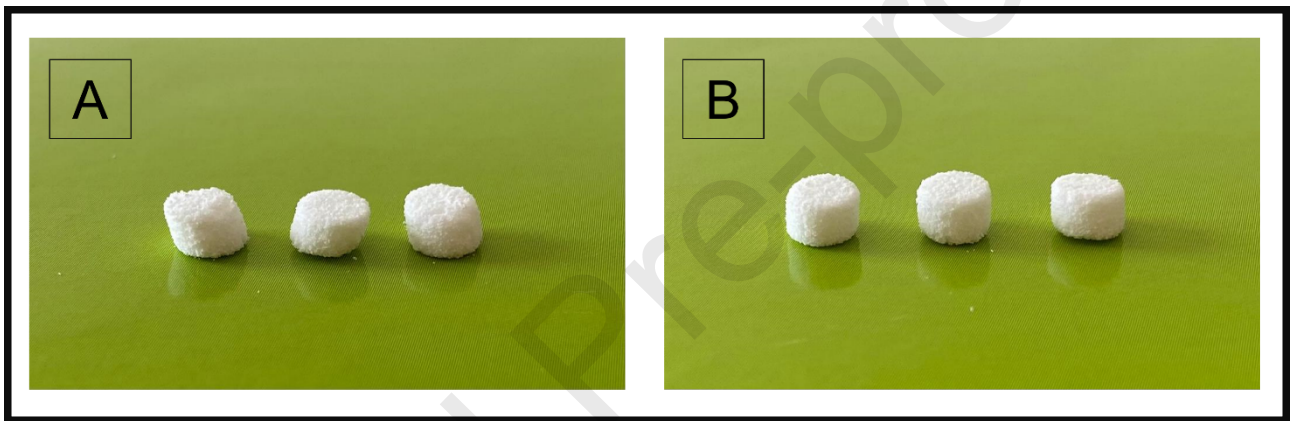


Figure 8. Influence of spread speed on the shape of the prototype LUDb. A= 40%, B= 10%

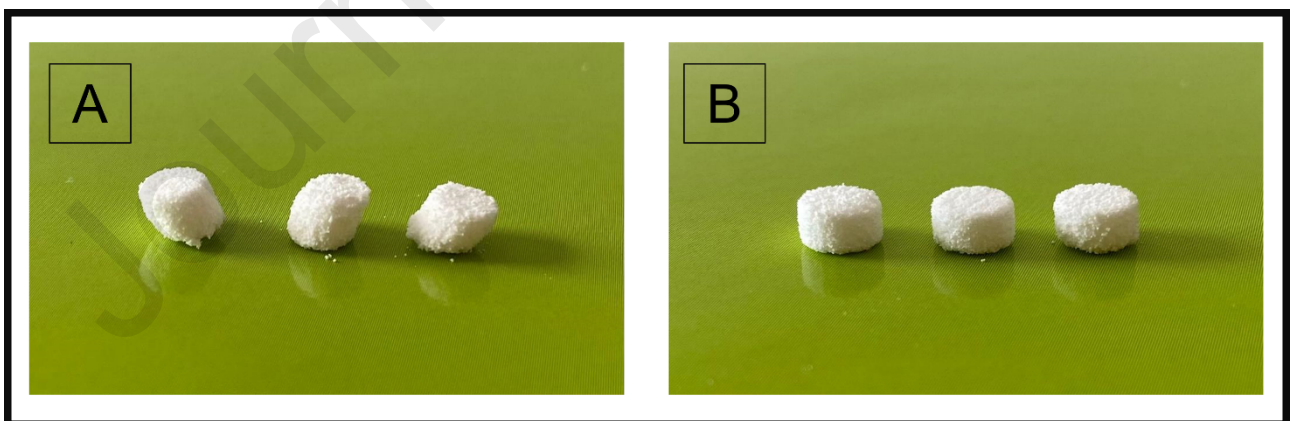


Figure 9. Influence of spread speed on the shape of the prototype PHAb. A= 40%, B= 10%

Figures 8 and 9 illustrate the photos of printed prototypes by using Wf2 and layer thickness of 0.2 mm, from LUDb and PHAb powder blends, respectively. In both cases, a reduction in the spread speed produced an improvement in the shape of the prototype, in fact, for the prototypes with LUDb, prepared with a speed of

10%, the shape improved from number 2 to number 0 and for those prepared with PHAb, the improvement was from 3 to 0.

The shape deformation underwent for the prototypes prepared with the higher roller speed (Figure 7B, 8B and 9B) may be because the binder solution was not completely absorbed when the successive layer was spread, so the roller dragged the underlying powder layer. Consequently, a decrease in the spread speed allowed the binder solution to be absorbed by the underlying powder before a second powder layer was deposited thus preventing the deformation of the printed prototype.

Conclusion

BJ-3D printing technology is an appropriate approach for the preparation of ODTs because it usually leads to the build-up of highly porous objects. Furthermore, it has the advantage of using well-known excipients for the preparation of solid dosage forms used in traditional manufacturing methods. To our knowledge, this study provides the first demonstration that co-processed excipients could be exploited to prepare orodispersible dosage forms by BJ-3D printing technology. Notably, the materials tested in this experimental work proved to be suitable to the aim proposed when mixed with excipients that improve the powder particle binding. The results confirmed the successful application of the materials, which have proved to be performing. For all studied co-processed materials, it has been observed that by changing the process parameters (i.e., layer thickness, waveform type, spread speed), prototypes with very different physical and mechanical characteristics were obtained. In particular, when the thickness of the layer decreased, the mechanical properties of the prototypes were improved probably because of the higher amount of binder solution added. The amount of liquid binder strongly affects the quality of the prototypes; in particular, when Wf1 was applied the prototypes were fairer and when Wf3 was set they were more deformed. Finally, the shape of the prototypes was improved when the spread speed was lower. These results highlight that a study of statistical optimization of the different process parameters and material attributes is required to develop ODT preparations endowed with good, reproducible and predictable technological properties (i.e., tablet morphology, friability, disintegration time, crushing strength). Moreover, the effect of a drying system during the printing process could be evaluated. The future development of this research project should also evaluate medicated formulation. On the horizon of the outcome of this work, a reappraisal of the unique potential of BJ-3D printer technology can be envisaged for the development of more feasible personalized pharmaceuticals.

Acknowledgements

This work was supported by NanoCosPha funds from Regione Lombardia and PNRR, MUSA project: Multilayered Urban Sustainability Action.

References

1. Ejeta F. Orally Disintegrating Tablets. In: Dosage Forms - Innovation and Future Perspectives. 2023.
2. Jang DJ, Bae SK, Oh E. Coated dextrin microcapsules of amlodipine incorporable into orally disintegrating tablets for geriatric patients. *Biomedicine and Pharmacotherapy*. 2014 Oct 1;68(8):1117–24.

3. Stoltenberg I, Breitzkreutz J. Orally disintegrating mini-tablets (ODMTs) – A novel solid oral dosage form for paediatric use. *European Journal of Pharmaceutics and Biopharmaceutics*. 2011 Aug 1;78(3):462–9.
4. Navarro V. Improving medication compliance in patients with depression: Use of orodispersible tablets. *Adv Ther*. 2010;27(11):785–95.
5. Llorca PM. Discussion of prevalence and management of discomfort when swallowing pills: Orodispersible tablets expand treatment options in patients with depression. *Ther Deliv*. 2011;2(5):611–22.
6. Cilurzo F, Musazzi UM, Franzé S, Selmin F, Minghetti P. Orodispersible dosage forms: biopharmaceutical improvements and regulatory requirements. *Drug Discov Today [Internet]*. 2018;23(2):251–9. Available from: <http://dx.doi.org/10.1016/j.drudis.2017.10.003>
7. Ghourichay MP, Kiaie SH, Nokhodchi A, Javadzadeh Y. Formulation and Quality Control of Orally Disintegrating Tablets (ODTs): Recent Advances and Perspectives. Yuksel N, editor. *Biomed Res Int [Internet]*. 2021 Dec 24;2021:1–12. Available from: <https://www.hindawi.com/journals/bmri/2021/6618934/>
8. Savini A, Savini GG. A short history of 3D printing, a technological revolution just started. In: 2015 ICOHTEC/IEEE International History of High-Technologies and their Socio-Cultural Contexts Conference (HISTELCON). IEEE; 2015. p. 1–8.
9. Martinez DW, Espino M, Cascolan HM, Crisostomo JL, Dizon JR. A Comprehensive Review on the Application of 3D Printing in the Aerospace Industry. *Key Eng Mater*. 2022;913 KEM:27–34.
10. Al Rashid A, Khan SA, G. Al-Ghamdi S, Koç M. Additive manufacturing: Technology, applications, markets, and opportunities for the built environment. *Autom Constr [Internet]*. 2020;118(June):103268. Available from: <https://doi.org/10.1016/j.autcon.2020.103268>
11. RANGEL B, GUIMARÃES AS, LINO J, SANTANA L. 3D Printing for Construction with Alternative Materials [Internet]. 2023. Available from: <https://link.springer.com/10.1007/978-3-031-09319-7>
12. Jamróz W, Szafraniec J, Kurek M, Jachowicz R. 3D Printing in Pharmaceutical and Medical Applications – Recent Achievements and Challenges. *Pharm Res [Internet]*. 2018 Sep 11;35(9):176. Available from: <http://link.springer.com/10.1007/s11095-018-2454-x>
13. Ahangar P, Cooke ME, Weber MH, Rosenzweig DH. Current biomedical applications of 3D printing and additive manufacturing. *Applied Sciences (Switzerland)*. 2019;9(8).
14. Fan D, Li Y, Wang X, Zhu T, Wang Q, Cai H, et al. Progressive 3D Printing Technology and Its Application in Medical Materials. *Front Pharmacol*. 2020;11(March):1–12.
15. Chen G, Xu Y, Kwok PCL, Kang L. Pharmaceutical Applications of 3D Printing. *Addit Manuf [Internet]*. 2020;34(March):101209. Available from: <https://doi.org/10.1016/j.addma.2020.101209>
16. Wang Y, Müllertz A, Rantanen J. Additive Manufacturing of Solid Products for Oral Drug Delivery Using Binder Jetting Three-Dimensional Printing. *AAPS PharmSciTech [Internet]*. 2022;23(6). Available from: <https://doi.org/10.1208/s12249-022-02321-w>
17. Vaz VM, Kumar L. 3D Printing as a Promising Tool in Personalized Medicine. Vol. 22, *AAPS PharmSciTech*. Springer Science and Business Media Deutschland GmbH; 2021.

18. Sun Y, Soh S. Printing Tablets with Fully Customizable Release Profiles for Personalized Medicine. *Advanced Materials*. 2015;27(47):7847–53.
19. Mostafaei A, Elliott AM, Barnes JE, Li F, Tan W, Cramer CL, et al. Binder jet 3D printing—Process parameters, materials, properties, modeling, and challenges. *Prog Mater Sci* [Internet]. 2021;119(May 2020):100707. Available from: <https://doi.org/10.1016/j.pmatsci.2020.100707>
20. Chen X, Wang S, Wu J, Duan S, Wang X, Hong X, et al. The Application and Challenge of Binder Jet 3D Printing Technology in Pharmaceutical Manufacturing. *Pharmaceutics*. 2022;14(12).
21. Sen K, Mehta T, Sansare S, Sharifi L, Ma AWK, Chaudhuri B. Pharmaceutical applications of powder-based binder jet 3D printing process – A review. *Adv Drug Deliv Rev* [Internet]. 2021;177:113943. Available from: <https://doi.org/10.1016/j.addr.2021.113943>
22. The world's first 3DP dosage form [Internet]. [cited 2023 Jul 21]. Available from: <https://www.aprecia.com/technology/zipdose>
23. Ziaee M, Crane NB. Binder jetting: A review of process, materials, and methods. Vol. 28, *Additive Manufacturing*. Elsevier B.V.; 2019. p. 781–801.
24. Derby B. Inkjet printing of functional and structural materials: Fluid property requirements, feature stability, and resolution. *Annu Rev Mater Res*. 2010;40:395–414.
25. Tai J, Gan HY, Liang YN, Lok BK. Control of Droplet Formation in Inkjet Printing Using Ohnesorge Number Category: Materials and Processes. In: 2008 10th Electronics Packaging Technology Conference [Internet]. IEEE; 2008. p. 761–6. Available from: <http://ieeexplore.ieee.org/document/4763524/>
26. Nachaegari SK, Bansal AK. Coprocessed Excipients for Solid Dosage Forms. *Pharmaceutical Technology*. 2004;28(1):52–64.
27. Challener CA. Development of Coprocessed Excipients. *Pharmaceutical Technology*. 2022;46(6).
28. Palugan L, Cerea M, Vecchio C, Maroni A, Foppoli A, Moutaharrik S, et al. Newly designed punch for scored tablets: Evaluation by an expert system based on quality by design. *J Drug Deliv Sci Technol*. 2021;65.
29. Infanger S, Haemmerli A, Iliev S, Baier A, Stoyanov E, Quodbach J. Powder bed 3D-printing of highly loaded drug delivery devices with hydroxypropyl cellulose as solid binder. *Int J Pharm* [Internet]. 2019 Jan 30;555(November 2018):198–206. Available from: <https://doi.org/10.1016/j.ijpharm.2018.11.048>
30. Antic A, Zhang J, Amini N, Morton DAV, Hapgood KP. Screening pharmaceutical excipient powders for use in commercial 3D binder jetting printers. *Advanced Powder Technology* [Internet]. 2021 Jul;32(7):2469–83. Available from: <https://doi.org/10.1016/j.apt.2021.05.014>
31. Wilts EM, Ma D, Bai Y, Williams CB, Long TE. Comparison of Linear and 4-Arm Star Poly(vinyl pyrrolidone) for Aqueous Binder Jetting Additive Manufacturing of Personalized Dosage Tablets. *ACS Appl Mater Interfaces* [Internet]. 2019 Jul 10;11(27):23938–47. Available from: <https://pubs.acs.org/doi/10.1021/acsami.9b08116>
32. Chang SY, Jin J, Yan J, Dong X, Chaudhuri B, Nagapudi K, et al. Development of a pilot-scale HuskyJet binder jet 3D printer for additive manufacturing of pharmaceutical tablets. *Int J Pharm* [Internet]. 2021 Aug;605(April):120791. Available from: <https://doi.org/10.1016/j.ijpharm.2021.120791>

33. Wang Z, Han X, Chen R, Li J, Gao J, Zhang H, et al. Innovative color jet 3D printing of levetiracetam personalized paediatric preparations. *Asian J Pharm Sci.* 2021 May 1;16(3):374–86.

